Nonimaging speckle interferometry for high-speed nanometer-scale position detection

E. G. van Putten,[1,3,*] A. Lagendijk,[1,2] and A. P. Mosk[1]

[1]*Complex Photonic Systems, Faculty of Science and Technology and MESA+ Institute for Nanotechnology, University of Twente, P.O. Box 217, 7500 AE Enschede, The Netherlands*

[2]*FOM Institute for Atomic and Molecular Physics, Science Park 104, 1098 XG Amsterdam, The Netherlands*

[3]*Current address: Philips Research Laboratories, 5656 AE Eindhoven, The Netherlands*
**Corresponding author: E.G.vanPutten@alumnus.utwente.nl*

Received November 21, 2011; revised February 8, 2012; accepted February 11, 2012;
posted February 13, 2012 (Doc. ID 158432); published March 12, 2012

We experimentally demonstrate a nonimaging approach to displacement measurement for complex scattering materials. By spatially controlling the wavefront of the light that incidents on the material, we concentrate the scattered light in a focus on a designated position. This wavefront acts as a unique optical fingerprint that enables precise position detection of the illuminated material by simply measuring the intensity in the focus. By combining two fingerprints we demonstrate position detection along one in-plane dimension with a displacement resolution of 2.1 nm. As our approach does not require an image of the scattered field, it is possible to employ fast nonimaging detectors to enable high-speed position detection of scattering materials.
OCIS codes: 120.3940, 290.0290.

Light is an ideal tool to perform contact-free, nondestructive, and high-precision metrology [1]. For this reason, optical positioning techniques have proven themselves indispensable in various branches of science and many important industrial processes, including the fabrication of semiconductor-based circuits with features on the nanometer regime. Fast feedback is essential in these high-precision positioning systems as high frequency vibrational motion limits the level of precision that these techniques offer.

In reflecting systems, laser interferometry [2,3] combined with high-speed detectors offers precise out-of-plane displacement measurements with a large bandwidth. For in-plane displacements, several speckle-based metrology techniques, such as speckle photography [4,5] and speckle interferometry [6–9], were developed in the late 1960s and 1970s [10]. These techniques spatially image speckle patterns to offer versatile measurements of material parameters, such as strain, displacement, and rotation [11]. However, the necessary spatial information limits the attainable bandwidth because these techniques require imaging detectors, which are orders of magnitude slower than nonimaging detectors, such as fast photodiodes, which can have gigahertz bandwidth.

Recent developments in optics [12–15] enabled control of the propagation of scattered light. These techniques, which are conceptually related to phase conjugation [16,17] and time reversal [18], manipulate the wavefront of the incident light using spatial light modulators [19] to steer the scattered light, for example, in a spatial and/or temporal focus at any desired position [12,20–23].

In this Letter we describe and experimentally demonstrate a nonimaging approach to displacement measurement for complex scattering materials. We concentrate the light that is scattered from the material in a sharp focus by spatially shaping the wavefront of the incident light. In a complex system lacking translational invariance, this wavefront acts as a unique optical fingerprint of the illuminated part of the sample. Any displacement between the fingerprint and the system reduces their overlap, thereby inevitably decreasing the intensity in the constructed focus. This dependence opens the possibility to use such fingerprints for position detection of the illuminated sample at resolutions of the order of nanometers. In our experiment we employed a CCD camera as a detector. However, as spatial information of the scattered field is no longer required, this method, furthermore, enables the use of fast detectors.

In Fig. 1 we have depicted our method to detect sample displacements. With a wavefront synthesizer, we spatially control the phase of a light beam. A detector behind

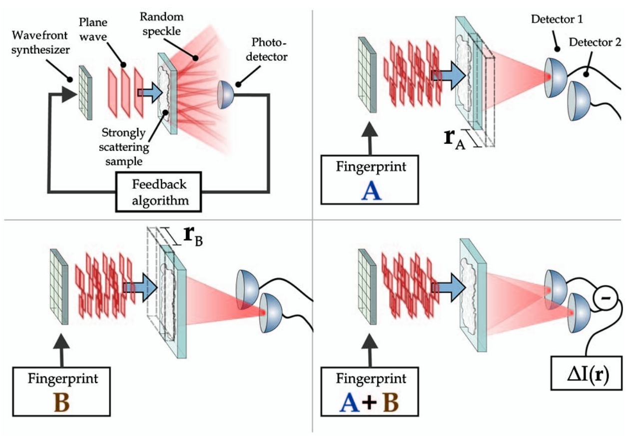

Fig. 1. Method to detect sample displacements. Light modulated by a wavefront synthesizer is projected on a scattering sample by a microscope objective (not shown). At the back of the sample a microscope objective (not shown) captures the scattered light. A detector coupled to the wavefront synthesizer monitors the scattered light in the Fourier plane of the sample surface. Two optical fingerprints are generated for two sample positions. Each of the fingerprints redirects the scattered light onto one of the detectors. The sample position **r** is determined by illuminating the sample with a superposition of the fingerprints and monitoring the intensity difference ΔI between the two detectors. While this figure shows a horizontal displacement, the method is more generally valid and can be made to work in all directions.

0146-9592/12/061070-03$15.00/0

a scattering sample combined with a feedback-based algorithm finds the fingerprint that focuses the transmitted light onto the detector [24]. We use this system to find the fingerprints A and B corresponding to two different sample positions, $\mathbf{r}_A$ and $\mathbf{r}_B$. In our current setup, this process takes several minutes. However, recently it has been shown [15,25] that such fingerprints can be found well within a second. Fingerprint A focuses the light onto the first detector when the sample is positioned at $\mathbf{r}_A$, while fingerprint B is constructed to concentrate the light onto the second detector when the sample is at $\mathbf{r}_B$. When we now position the sample in between $\mathbf{r}_A$ and $\mathbf{r}_B$, while illuminating it with a wavefront that is constructed by coherently summing complex amplitudes of fingerprints A and B, the sample position can be interpolated from the intensity difference of the two detectors. This method can be easily extended to detect displacements in multiple directions by generating multiple optical fingerprints at different sample positions.

The sensitivity of this detection method and the corresponding smallest measurable displacement $\delta\mathbf{r}$ are determined by the way the intensities I_A and I_B in the two foci change under a sample displacement. When the sample is illuminated by an optical fingerprint, the focus intensity I_0 is a function of the sample displacement $\Delta\mathbf{r} \equiv \mathbf{r} - \mathbf{r}_0$ from its original position $\mathbf{r}_0$:

$$I_0(\Delta\mathbf{r}) = \eta\langle I_{\mathrm{bg}}\rangle\langle|\gamma(\Delta\mathbf{r})|^2\rangle, \tag{1}$$

where $\langle\cdot\rangle$ denotes ensemble averaging over disorder. The enhancement factor η is defined as the ratio between the intensity $I_0(0)$ and the ensemble averaged background intensity $\langle I_{\mathrm{bg}}\rangle$. This enhancement depends linearly on the number of degrees of freedom in the wavefront [12]. The value of $\langle|\gamma(\Delta\mathbf{r})|^2\rangle$ accounts for the loss in overlap between the sample and the optical fingerprint under sample displacement.

When the range of complexity in the sample is on a subwavelength scale, the overlap of the optical fingerprint with the sample depends solely on the illumination optics. In our experiment, the pixels of the wavefront synthesizer are projected onto the back aperture of an infinity corrected microscope objective. In this geometry, we calculated the overlap using the formalism of [10] for an in-plane lateral displacement to yield

$$\langle|\gamma(\Delta\mathbf{r})|^2\rangle = \left[\frac{2J_1(k_{\max}|\Delta\mathbf{r}|)}{k_{\max}|\Delta\mathbf{r}|}\right]^2, \tag{2}$$

where the maximum contributing transversal wave vector $k_{\max}$ is determined by the NA of the microscope objective, $k_{\max} = 2\pi\mathrm{NA}/\lambda$. This overlap only equals unity for $\Delta\mathbf{r} = 0$ and becomes smaller for any nonzero displacement.

The highest sensitivity of the systems is found by maximizing the gradient ∇ of the difference intensity $\Delta I \equiv I_B - I_A$. By using Eqs. (1) and (2), we find the maximum value of this gradient exactly in between $\mathbf{r}_A$ and $\mathbf{r}_B$ when their distance is set to $|\mathbf{r}_A - \mathbf{r}_B|_{\mathrm{opt}} = 2.976/k_{\max}$. For these conditions, the resulting optimal sensitivity S_{opt} is

$$S_{\mathrm{opt}} \equiv \max[\nabla(\Delta I)] = \frac{5.8\mathrm{NA}\eta}{\lambda}\langle I_{\mathrm{bg}}\rangle. \tag{3}$$

By changing the enhancement η, the wavelength λ, and the NA of the optics, it is possible to tune the sensitivity over a wide range.

To test our position detection method we employ a spatial light modulator (SLM) from Holoeye (LC-R 2500) that allows us to spatially modulate the phase of a beam from a cw laser (Coherent Compass M315–100, $\lambda = 532$ nm). The modulated beam is then imaged onto the back aperture of a microscope objective (NA $= 0.95$). In the focal plane of the microscope objective we have placed a strongly scattering sample on top of a high-precision positioning xyz stage (PI P-611.3S NanoCube). The sample is composed of zinc oxide powder on top of a glass cover slide. At the back of the sample we collect the transmitted light and image the far field of the sample surface onto a CCD camera (Dolphin F-145B, 10 fps). As our method does not need a spatially imaging detector, the camera can be replaced with two photodiodes to maximize bandwidth.

The optimal distance between optimization positions $\mathbf{r}_A$ and $\mathbf{r}_B$ is calculated to be 252 nm for this system. Without loss of generality, we consider only lateral translations in the x direction. We define the original sample position as $x_0 = 0$ nm. The sample is translated toward $x_A = -126$ nm. A feedback-based algorithm finds the optical fingerprint for which the scattered light is focused on the left side of the camera. Then we position the sample at $x_B = +126$ nm and repeat the procedure to create a focus on the right side of the camera. The two fingerprints are superimposed on the SLM. When we move the sample back to the original position x_0, the two spots become visible on the camera.

In Fig. 2 the intensity in the two spots as a function of the sample displacement $\Delta x \equiv x - x_0$ is plotted, together with camera images for three different values of Δx. The two curves denote the intensity behavior predicted by Eqs. (1) and (2) without free parameters. Starting from $\Delta x = 0$, where the intensity in both spots is equal, I_A and I_B change differently under sample displacement. Moving the sample in the positive x direction results

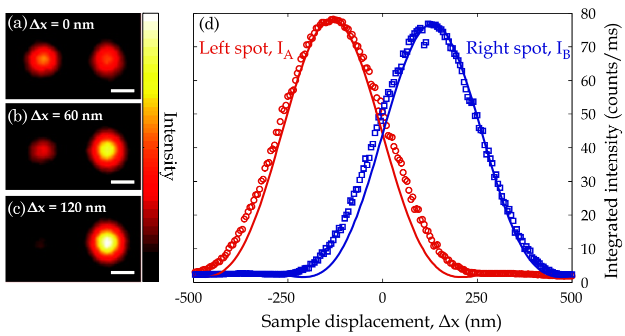

Fig. 2. Spot intensities as function of the sample displacement. (a)–(c) Camera images for different values of the sample displacement Δx. The scale bars denote 1 mm. (d) Measured spot intensities (circles I_A, squares I_B) as function of the sample displacement. The solid curves denote the theoretical expected behavior. One count on our detector is equal to an amount of photoelectrons of the order of 10.

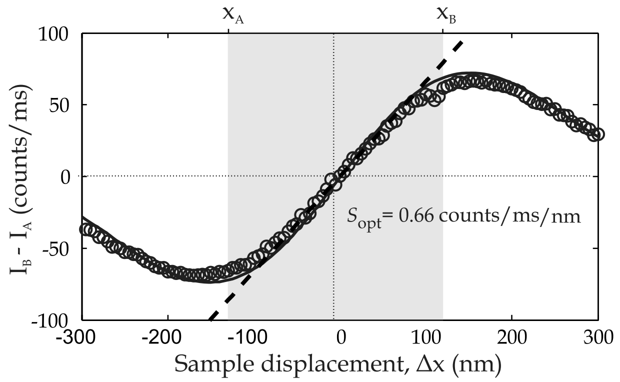

Fig. 3. Intensity difference $I_B - I_A$ as a function of the sample displacement Δx. The circles denote the measured intensity difference, while the solid curve represents the theoretical intensity difference. Within the gray area the function is bijective. The dotted line is a linear fit to the data points close to $\Delta x = 0$. From the fit we find that the slope equals $S_{opt} = 0.66$ counts/ms/nm.

in a decreasing I_A, while I_B increases for $\Delta x < x_B$. The experimental data is in good agreement with theory, although the measured intensity dependence is slightly wider. This small deviation is likely to be caused by a nonideal transfer function of the optics, which cannot be compensated for by wavefront corrections.

To find the position of the sample from the measured data, we look at the difference intensity between the two spots, which is plotted in Fig. 3. For $x_A < \Delta x < x_B$ (gray area) the function is bijective, resulting in a unique mapping between the difference signal and the sample position. Over a large distance, the function is linear and only close to the displacements $\Delta x = x_A$ and $\Delta x = x_B$ does the function start to curve. The highest sensitivity is found at $\Delta x = 0$, where the slope has a maximum value of $S_{opt} = 0.66$ counts/ms/nm, close to the theoretical limit for this system of 0.80 cnts/ms/nm that we calculated using Eq. (3). The noise level in our setup is found to be 1.42 counts/ms, so that the achievable displacement resolution is 2.1 nm. We know that part of the noise may, in fact, be signal, i.e., fluctuations of the actual sample position. The achieved resolution compares favorably with state-of-the-art techniques [26]. A higher resolution is possible by increasing the signal-to-noise ratio in the system [27].

Instead of measuring the scattered light in transmission, one could also choose to work in reflection. Furthermore, by employing more than two detectors and generating multiple optical fingerprints, the method can be expanded in a straightforward way to simultaneously detect displacements in multiple directions. Similarly, the optical fingerprints can also be configured to detect other sample movements, such as rotations. This flexibility makes our technique very suitable for high-speed and high-precision position monitoring of complex scattering structures.

The authors thank I. M. Vellekoop and W. L. Vos for their valuable support. I. D. Setija from ASML Netherlands B.V. is acknowledged for stimulating discussions. A. P. Mosk is supported by a Vidi grant from the Netherlands Organization for Scientific Research (NWO).

References

1. K. J. Gåsvik, *Optical Metrology* (Wiley, 2002).
2. N. Bobroff, Meas. Sci. Technol. **4**, 907 (1993).
3. R. J. Dewhurst and Q. Shan, Meas. Sci. Technol. **10**, R139 (1999).
4. J. M. Burch and J. M. J. Tokarski, Opt. Acta **15**, 101 (1968).
5. E. Archbold, J. M. Burch, and A. E. Ennos, Opt. Acta **17**, 883 (1970).
6. J. A. Leendertz, J. Phys. E **3** (1970).
7. J. Butters and J. Leendertz, Opt. Laser Technol. **3**, 26 (1971).
8. A. Macovski, S. D. Ramsey, and L. F. Schaefer, Appl. Opt. **10**, 2722 (1971).
9. O. Lekberg, Phys. Technol. **11**, 16 (1980).
10. J. W. Goodman, *Speckle Phenomena in Optics* (Roberts, 2006).
11. G. H. Kaufmann, ed., *Advances in Speckle Metrology and Related Techniques* (Wiley, 2011).
12. I. M. Vellekoop and A. P. Mosk, Opt. Lett. **32**, 2309 (2007).
13. S. M. Popoff, G. Lerosey, R. Carminati, M. Fink, A. C. Boccara, and S. Gigan, Phys. Rev. Lett. **104**, 100601 (2010).
14. T. Čižmár, M. Mazilu, and K. Dholakia, Nat. Photon. **4**, 388 (2010).
15. Y. Choi, T. D. Yang, C. Fang-Yen, P. Kang, K. J. Lee, R. R. Dasari, M. S. Feld, and W. Choi, Phys. Rev. Lett. **107**, 023902 (2011).
16. E. N. Leith and J. Upatnieks, J. Opt. Soc. Am. **56**, 523 (1966).
17. Z. Yaqoob, D. Psaltis, M. S. Feld, and C. Yang, Nat. Photon. **2**, 110 (2008).
18. M. Fink, D. Cassereau, A. Derode, C. Prada, P. Roux, M. Tanter, J.-L. Thomas, and F. Wu, Rep. Prog. Phys. **63**, 1933 (2000).
19. C. Maurer, A. Jesacher, S. Bernet, and M. Ritsch-Marte, Laser Photon. Rev. **5**, 81 (2011).
20. I. M. Vellekoop, E. G. van Putten, A. Lagendijk, and A. P. Mosk, Opt. Express **16**, 67 (2008).
21. J. Aulbach, B. Gjonaj, P. M. Johnson, A. P. Mosk, and A. Lagendijk, Phys. Rev. Lett. **106**, 103901 (2011).
22. O. Katz, E. Small, Y. Bromberg, and Y. Silberberg, Nat. Photon. **5**, 372 (2011).
23. D. J. McCabe, A. Tajalli, D. R. Austin, P. Bondareff, I. A. Walmsley, S. Gigan, and B. Chatel, Nat. Commun. **2**, 447 (2011).
24. I. M. Vellekoop and A. P. Mosk, Opt. Commun. **281**, 3071 (2008).
25. M. Cui, Opt. Express **19**, 2989 (2011).
26. G. Pedrini, J. Gaspar, M. E. Schmidt, I. Alekseenko, O. Paul, and W. Osten, Opt. Eng. **50**, 101504 (2011).
27. J. W. Wagner and J. B. Spicer, J. Opt. Soc. Am. B **4**, 1316 (1987).